A&A 371, 986–996 (2001)
DOI: 10.1051/0004-6361:20010462

Astronomy & Astrophysics

Fourier decomposition and frequency analysis of the pulsating stars with $P < 1$ d in the OGLE database

I. Monoperiodic Delta Scuti, RRc and RRab variables. Separation criteria and particularities*

E. Poretti**

Osservatorio Astronomico di Brera, Via E. Bianchi 46, 23807 Merate, Italy

Received 26 January 2001 / Accepted 14 March 2001

Abstract. The OGLE database is revisited to investigate in more detail the properties of the Fourier parameters. Methodological improvements led us to identify a clear separation among High–Amplitude δ Scuti (HADS), RRc and RRab stars. The bimodal distribution of the R_{21} parameter in HADS stars is explained as a contamination effect from RRc stars: there is evidence that all stars with $0.20 < P < 0.25$ d are RRc variables. The previously claimed existence of a subclass of unusual HADS is demonstrated to be a spurious result. Candidate overtone pulsators are found among HADS and RRc variables. The properties of the Fourier parameters are discussed as a function of the physical conditions in the stars involved. Among the field RRab stars we detected different light–curve groups producing distinct "tails" in the Fourier plots for $P > 0.55$ d; evolutionary phases or the combination of different physical conditions (not only metallicity) are suggested to explain this separation, observed also in the cluster RRab stars. The stellar parameters of RRc stars in a given globular cluster show different tendencies than those of RRc stars from different clusters.

Key words. methods: data analysis – techniques: photometric – astronomical data bases: miscellaneous – stars: oscillations – stars: variables: δ Sct – stars: variables: RR Lyr

1. Introduction

The *Optical Gravitational Lensing Experiment* (OGLE; Udalski et al. 1993) is a project whose main goal is a systematic search for microlensing events. As a valuable by–product, a large amount of photometric data was acquired on a variety of variable stars. As demonstrated by several studies, the light curves of pulsating stars depend on their physical parameters. Moreover, the observed light curves can be compared with those derived from hydrodynamic pulsational models. Therefore, once an observable quantity has been recognized as depending on stellar parameters, it is possible and useful to fix the relation between this quantity and the light curve. That can help us in obtaining stellar parameters for stars for which we have only light curves, i.e. the by-product of the microlensing projects.

The Fourier decomposition is a powerful method to describe in a synthetic and safe way the shape of a light curve. It consists in fitting the photometric measurements by means of the series

$$I(t) = A_{\rm o} + \sum_{i=1}^{N} A_i \cos[2\pi i(t - T_{\rm o})f + \phi_i] \qquad (1)$$

where $I(t)$ is the magnitude observed at time t, A_0 the mean magnitude, A_i the amplitude of the i–component (the $i-1$ harmonic), f the frequency ($f = 1/P$, where P is the period of the light variation), ϕ_i the phase of the i–component at $t = T_{\rm o}$.

The Fourier parameters can be subdivided into two groups: the amplitude ratios $R_{ij} = A_i/A_j$ (i.e. $R_{21} = A_2/A_1$, $R_{31} = A_3/A_1$, $R_{32} = A_3/A_2$, ...) and the phase differences $\phi_{ji} = i\phi_j - j\phi_i$ (i.e. $\phi_{21} = \phi_2 - 2\phi_1$, $\phi_{31} = \phi_3 - 3\phi_1$, $\phi_{32} = 2\phi_3 - 3\phi_2$, ...). Note that the use of the `sin` term instead of the `cos` leads to results that are not directly comparable, owing to the $\pi/2$ shift of each component. Because it provides quantitativeparameters to define the

* Tables 3, 4 and 5 are only available in electronic form at the CDS via anonymous ftp to
`cdsarc.u-strasbg.fr (130.79.128.5)` or via
`http://cdsweb.u-strasbg.fr/cgi-bin/qcat?J/A+A/371/986`
or via e-mail from the author.

** e-mail: `poretti@merate.mi.astro.it`

shape of the light curves, the Fourier decomposition is a suitable tool for classification purposes, once care is taken to avoid spurious results or misinterpretations of features of the light curves. Moreover, the plots of the Fourier parameters versus periods showed the presence of discontinuities in the progressions, which can be ascribed to resonances between different pulsational modes, as in the case of Classical Cepheids at $P \sim 10$ d. These diagrams are therefore useful tools to perform asteroseismology in giant stars, as the Cepheids (Poretti 2000a), even if some caution is necessary to locate exactly the position of the resonances (see Kienzle et al. 1999 and Feuchtinger et al. 2000 for a discussion of the resonance between the fourth and first overtones in the case of s–Cepheids).

In this paper, we examine the Fourier plots of the pulsating stars with period less than 1 d contained in the OGLE database in order to emphasize their properties.

2. The OGLE database

We considered the 268 pulsating stars included in the 15 fields covered by the OGLE database. The number of stars is large enough to constitute a conspicuous sample, able to provide unambiguous characterizations of these variables, and small enough to allow a star-by-star analysis, thus avoiding the misinterpretations that could arise from automated analysis. Each light curve is suitable to be Fourier decomposed thanks to the high number of homogeneous measurements (with a few exceptions) and we expected a clear detection of features and peculiarities, both for individual stars and for classes of variables. The analysis consisted of the separate steps described in the next subsections.

2.1. The verification of previous results

The primitive idea was simply to investigate the Fourier plots obtained by Morgan et al. (1998a, 1998b, 1998c) to clarify some ambiguous patterns. In particular, the $\phi_{31}-P$ plot does not show any clear progression; the $\phi_{21}-P$ plot also shows a strange scatter at short periods. If these results were confirmed, they should be considered as a failure of the capabilities offered by the Fourier decomposition as a sharp tool to describe light curves.

A close examination of the coefficients of the least–squares fit reported by Morgan et al. (1998a, 1998b, 1998c) reveals that in many cases the small amplitude terms are not significant, the error bars being as large as the amplitudes themselves. In other cases, the presence of large–amplitude high–order harmonics (i.e. $A_{i+1}/A_i \sim 1$) implies a really odd fitting light curve with humps and bumps. In general, $A_{i+1}/A_i < 0.5$ should be the rule far from resonances. Only the necessity of fitting the double maximum of RRc variables, the well–defined humps at minimum light of some RR Lyr variables or very asymmetrical curves should involve deviations from this rule, generating a few consecutive terms having similar amplitudes. Therefore, we matured the idea that a re–analysis of all the datasets was necessary to handle more reliable Fourier coefficients. At this point, we were forced to scrutinize each star again.

2.2. The fit of the OGLE light curves

We excluded 6 stars from the original sample (BW1_V31, BW9_V55, BWC_V22, BWC_V28, BWC_V97 and BWC_V56). For these stars, the number of measurements is less than 60 and the fit is quite uncertain, hampering a reliable determination of the Fourier parameters. In 8 other cases the measurements do not show significant deviations from a perfect sine–shaped light curve, probably owing to the small amplitude: BW1_V90 (full–amplitude 0.08 mag), BW2_V44 (0.10 mag), BW4_V55 (0.04 mag), BW4_V94 (0.06 mag), BW5_V117 (0.10 mag), BW6_V120 (0.10 mag), BW7_V74 (0.05 mag) and MM5-B_V141. It should be noted that 0.049 d $< P <$ 0.180 d for all these stars (and for 6 of them $P <$ 0.10 d): the shorter periods are compatible with the possibility that these stars are overtone pulsators. Figure 1 shows a light curve in which it was not possible to detect the amplitude and phase values of the first harmonic in a reliable way. Morgan et al. (1998c) considered four of these variables (BW1_V90, BW4_V94, BW6_V120, BW7_V74; see their Table 1) as unusual δ Sct. This misleading conclusion was due to the over–evaluation of the significance of their ϕ_{21}, ϕ_{31}, ϕ_{41} parameters.

In 8 more cases (BW1_V7, BW4_V132, BW5_V135, BW5_V174, BW9_V35, BW10_V39, BWC_V65 and MM7-B_V7) it was not possible to apply the Fourier decomposition: a high–order fit was requested to interpolate the measurements describing a very asymmetric shape, but the result is an improbable curve with evident bumps. In such cases the combination of the noise with the large number of free parameters is responsible for the unacceptable (from an astrophysical point of view) curve, even if the least–squares routine brings out figures. The frequency analysis did not reveal any second periodicity. Figure 2 shows an example.

Finally, we reduced to 246 the number of stars whose light curves were able to be decomposed. The 22 stars we rejected can be considered as partially responsible for the unclear Fourier plots obtained by Morgan et al. (1998a, 1998b, 1998c). In particular, this led us to a first specific result. We had already found that 4 of the stars described by Morgan et al. (1998c) as unusual δ Sct stars have a sine–shaped light curve. Proceeding further, we found that the curves of all the remaining "unusual" stars could be fitted by a $M = 2$ Fourier series and hence the ϕ_{31} and ϕ_{41} values don't have any significance. Since the ϕ_{21} parameters of these remaining stars assume quite normal values, the claimed subclass of unusual δ Sct stars previously reported doesn't exist.

Moreover, we changed the decomposition order M of about 70% of stars; in this way the Fourier plots involving high–order terms improved in clearness.

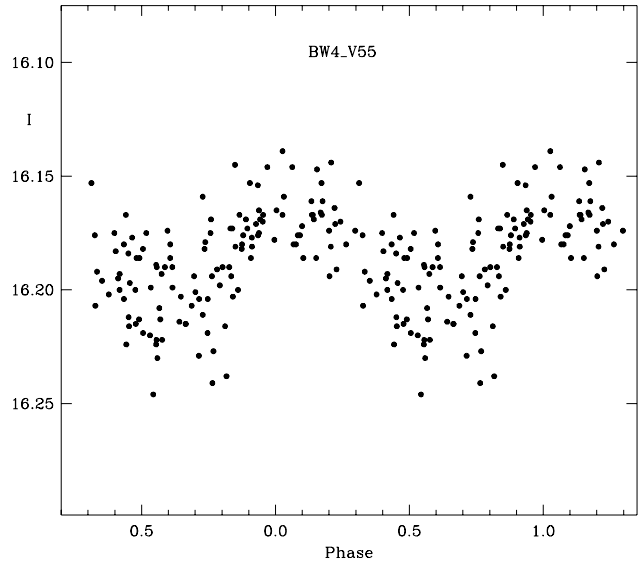

Fig. 1. Example of a sine–shaped light curve (BW4_V55, $P = 0.15958$ d). The small amplitude (the fitting curve has a full amplitude of 0.04 mag) and the noise (rms residual 0.016 mag) do not allow the detection of a significant first harmonic contribution

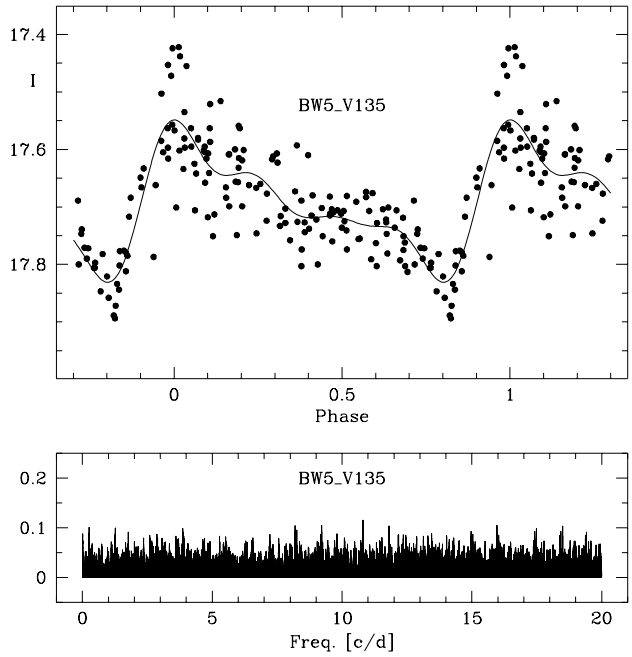

Fig. 2. Top panel: example of an unacceptable least–squares fit (BW5_V135, $P = 0.58825$ d). It is hard to believe that the bumps are real; the asymmetry of the light curve requires a high order of the Fourier fit ($M = 4$) and the large scatter enhances the amplitude of the high–order terms. Bottom panel: the power spectrum of the residuals does not show any significant second periodicity

2.3. The period refinement

The Fourier decomposition of the light curves by a single frequency (plus harmonics) could not always give a satisfactory fit, sometimes leaving a high rms residual. In such cases, it is quite obvious to investigate the datasets searching for other periodicities; this examination had not been done in the previous analysis. In many cases our frequency analysis revealed the presence of other peaks in the power spectrum. Since most of these peaks are observed very close to the main one and since such periods are expected as signatures both of nonradial oscillations and of a Blazhko effect, we must be sure that the reported periods are accurate. If not, a wrong period can generate spurious alias peaks or change the observed value of the neighbouring real peaks.

Therefore, we decided to refine the periods of all the stars and then to re-analyze in frequency all the datasets. To this end, we considered as preliminary solutions the least–squares fit obtained by using the period values reported in the OGLE database and the order M established in the previous step. This solution was given as input parameters to a code keeping locked the relations between the main frequency and the harmonic terms (MTRAP; Carpino et al. 1987); the best fit was searched for around the preliminary solution. Once the correct period was obtained, we re–examined in frequency all the datasets to detect secondary periodicities. No prewhitening was done: only the frequency values of the main term and its harmonics were considered as input values (known constituents), not their amplitude and phase. This approach is the same as the one used by Pardo & Poretti (1997) to detect the frequency content of double–mode Cepheids. The period refinement was marginal in most cases: for 73 stars (30% of the sample) it is smaller than 1 10^{-6} d, for 168 stars (72% of the sample) is smaller than 5 10^{-6} d. The mean error on the period is 1.3 10^{-6} d and for about 100 stars out of 234 the refinement was made within this error bar. As a by-product, we made a further revision of the significance of the small amplitude terms. The main result of this search is described in the next subsection.

2.4. The different frequency content of pulsating variables

At the end of this step we separated the monoperiodic variables from the other stars. Of course, a second, small-amplitude term may always be hidden in the noise, even if the fit with a single–period looks satisfactory. However, after the further check we made, we can be confident that its effect on the main period should be negligible. As a result of the period refinement procedure and the subsequent frequency analysis, we evidenced 53 stars showing a well–established multimode behaviour:

1. double–mode stars pulsating in the fundamental radial mode and in another radial overtone (7 candidates), with a well–separated pair of frequencies;
2. stars showing one single peak close to the main frequency (30 candidates), with a ratio $f_1/f_2 \sim 0.99$ or $\sim$1.01;

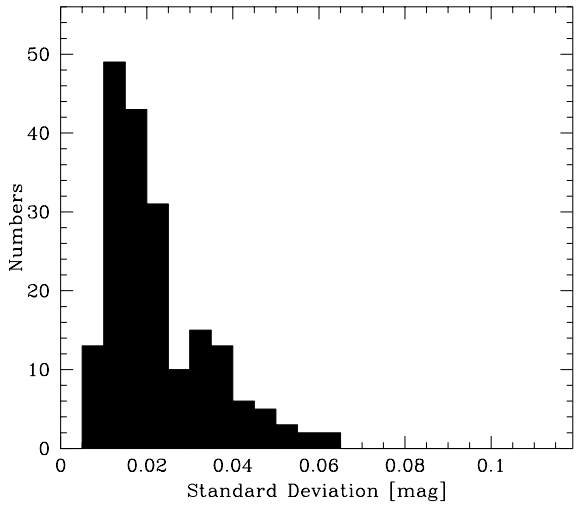

Fig. 3. Histogram of the standard deviations of the reliable Fourier fits of the light curves of the 192 monoperiodic stars

3. stars showing two peaks symmetric with respect to the main frequency and, in some cases, to the harmonics (7 candidates);
4. stars showing a second peak very close to the main one (9 candidates), $f_1/f_2 \sim 0.999$ or $\sim$1.001, suggesting a period variation or an unresolved, very long Blazhko effect.

All these types of multimode variables will be discussed in forthcoming papers. Not considering the Pop. II Cepheid BWC_V1 ($P = 1.74797$ d), we got a reliable Fourier decomposition of 192 monoperiodic variables with $P < 1$ d. In general, the fit is satisfactory even if some light curves appeared to be noisy. That can be ascribed both to difficult image reduction (close companion, nearby bright stars, ...) or to slow instrumental drifts, which appear in the frequency analysis as peaks very close to 0.000 cd^{-1} or 1.000 cd^{-1}. In 136 cases (i.e. the 71%) the least–squares fits have a standard deviation better than 0.03 mag (Fig. 3), a value quite acceptable for stars of I–magnitude 15–17 measured on a time baseline of three years.

We would like to emphasize the fact that all the work described above constitutes a complete independent re–analysis of the whole OGLE database. The new multiperiodic pulsators we found, the sharper revision of the light curve fits and the elimination of unclear subclasses of variables configure our Fourier analysis of the OGLE database as a very reliable tool to investigate the properties of the pulsating variables with $P < 1$ d.

3. The Fourier diagrams: the separations between variable classes

We can finally handle the well–defined Fourier plots shown in Figs. 4, 5, 6 and 7. Table 1 lists the averaged errors on the Fourier parameters for each class, as calculated from the errors on the least–squares fits.

Considering $P < 1$ d, the pulsating stars should be subdivided into High–Amplitude δ Scuti (HADS), RRc and RRab stars. However, the continuity of the progressions of the phase parameters (Figs. 4, 5, 6) masks the separation between HADS and RRc stars. Such a subdivision is more appreciable in the $R_{21}-P$ plot (Fig. 7). As a first step, a close examination can help in separating variable classes more precisely. For the sake of clarity, the subdivisions are shown right away in Figs. 4, 5, 6 and 7 by means of different symbols.

Table 1. Averaged errors on the ϕ_{21}, ϕ_{31}, ϕ_{41} and R_{21} parameters

	ϕ_{21}	ϕ_{31}	ϕ_{41}	R_{21}
		[rad]		
HADS	0.23	0.34	0.41	0.05
RRc	0.16	0.24	0.33	0.02
RRab	0.05	0.07	0.12	0.02

3.1. HADS or RRc?

In the period range 0.15–0.25 d, separating an RRc variable from a HADS is not an easy task, since for example, the $\phi_{21}-P$ plot (Fig. 4) shows a merging of two families of points, without any apparent jump. However, the light curve of a star following the progression coming from the shortest period shows an asymmetrical light curve with a sharp maximum (BW6_V30, $P = 0.18902$ d; Fig. 8, top panel), while in the opposite direction we generally find more smoothed light curves with rounded maxima (BW9_V114, $P = 0.20767$ d, Fig. 8, bottom panel). If the difference is not quite evident in the $\phi_{21}-P$ and $\phi_{31}-P$ plots (Figs. 4 and 5), it can be better appreciated both in the $\phi_{41}-P$ plot (Fig. 6) and in the $R_{21}-P$ one (Fig. 7).

We didn't detect any A_4 term for stars in the 0.20 d $< P <$ 0.25 d interval, suggesting that the light curves are more sinusoidal: it looks natural to ascribe this feature to the rapid evolution of the light curves of RRc stars (see the steady slope of ϕ_{41} parameters for $P > 0.30$ d). In the latter, a well defined dip is observed in the interval from 0.20 to 0.40 d, suggesting that all these stars belong to the same family. In particular, note the $R_{21} > 0.2$ values for $P < 0.20$ d and the $R_{21} < 0.15$ for 0.20 d $< P <$ 0.25 d. We can conclude that the Fourier parameters of stars in the interval 0.20 d $< P <$ 0.25 d are naturally linked with the longer periods (i.e. RRc stars) rather than with the shorter ones (i.e. HADS stars).

Another way to separate HADS from RRc stars is to plot the A_1^2 term versus the A_2 one (Fig. 9, see also Antonello 2000). There is some crowding close to the origin, but the two classes are well separated in the critical range 0.15–0.25 d.

Therefore, we have demonstrated that when dealing with a well–defined sample of accurate light curves, it is possible to separate HADS from RRc stars not on the basis of a mere assumption (Antonello 2000), but by looking at the amplitude values. We shall find below a further confirmation of this separation.

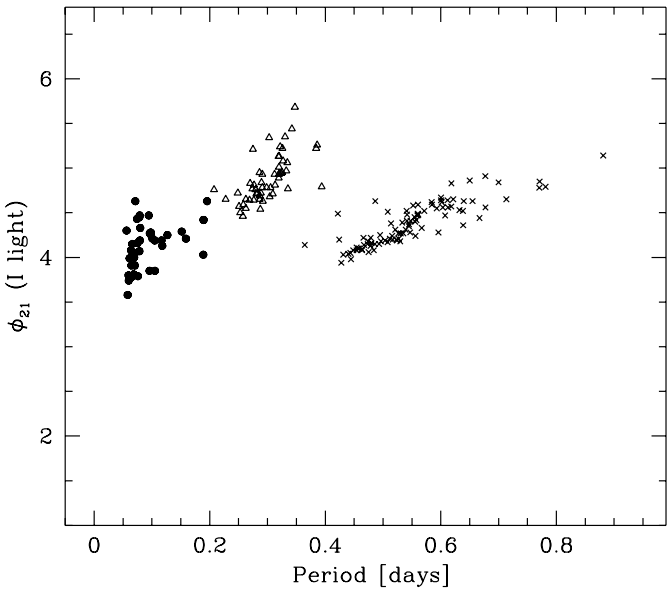

Fig. 4. Fourier parameter ϕ_{21} against Period for the 192 monoperiodic stars with $P < 1$ d in the OGLE database. Filled circles: HADS; open triangles: RRc; crosses: RRab stars

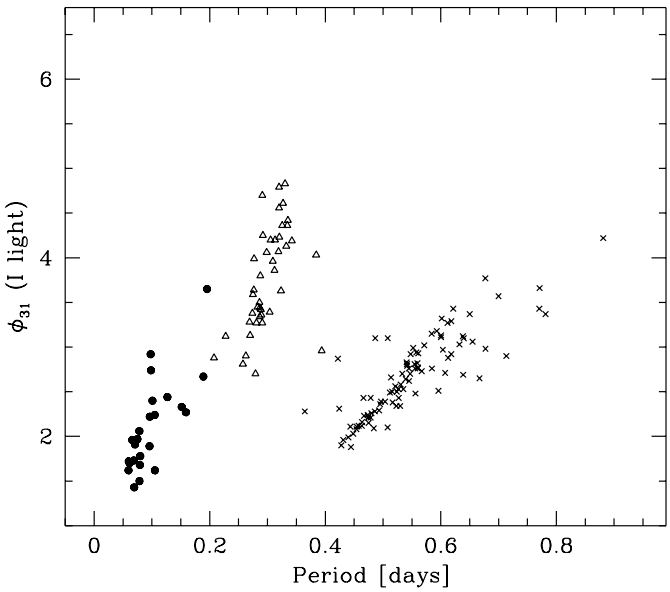

Fig. 5. Fourier parameter ϕ_{31} against Period for the 192 monoperiodic stars with $P < 1$ d in the OGLE database. Same symbols as in Fig. 4

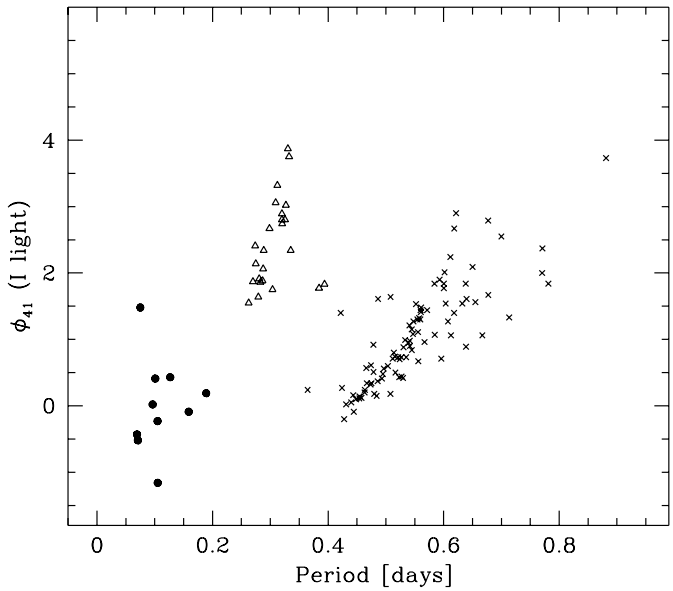

Fig. 6. Fourier parameter ϕ_{41} against Period for the 192 monoperiodic stars with $P < 1$ d in the OGLE database. Same symbols as in Fig. 4

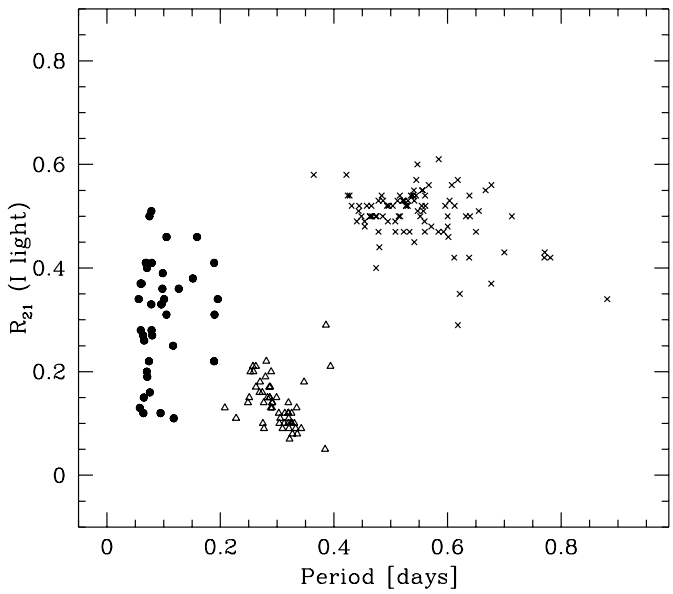

Fig. 7. Fourier parameter R_{21} against Period for the 192 monoperiodic stars with $P < 1$ d in the OGLE database. This plot yields the clearest separation between HADS and RRc stars. Same symbols as in Fig. 4

The separation between HADS and RRc stars by using $P = 0.20$ d as a clean cut cannot be considered as an inviolable rule; as an example, the symmetrical light curve of MM5-B_V141 ($P = 0.181$ d) suggests that this star belongs to RRc variables rather than to HADS. We also note that the presence of second overtone pulsators among RRc variables is always an open possibility; such pulsators should show more symmetrical light curves and the low R_{21} values observed here can be a hint.

3.2. RRc or RRab?

Looking at Fig. 4, RRc and RRab stars are clearly separated. In general, RRc stars have a period $P < 0.35$ d and for this period $\phi_{21} > 4.5$ rad; RRab stars have a period $P > 0.42$ d and for this period $\phi_{21} < 4.0$ rad. Similar separations can be found in all the phase and amplitude plots.

There are only a few exceptions, i.e. the presence of an isolated short–period RRab star, MM5-B_V31 ($P = 0.36456$ d) and of three long–period RRc stars,

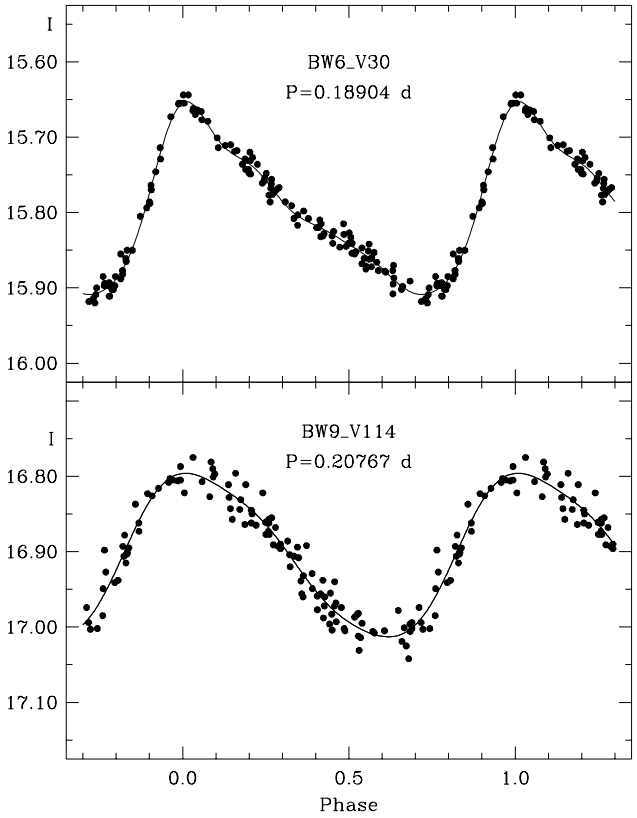

Fig. 8. Top panel: note the sharp maximum in the light curve of BW6_V30 (P = 0.18904 d), which can be considered the HADS with the longest period. Bottom panel: note the rounded maximum in the light curve of BW9_V114 (P = 0.20767 d), which seems to be the extreme short–period RRc

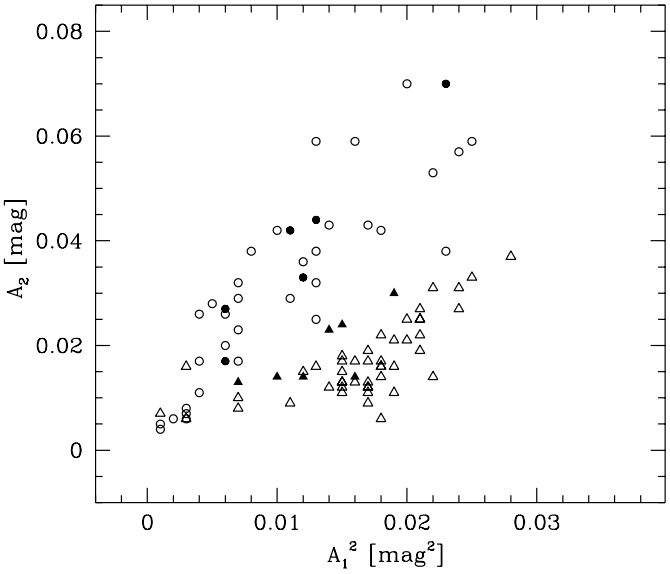

Fig. 9. The amplitudes of the first Fourier terms separate HADS (circles) from RRc (triangles) stars. Filled circles are HADS stars with $0.15 < P < 0.20$ d; filled triangles are RRc stars with $0.20 < P < 0.25$ d

BW1_V11 (P = 0.38434 d), BWC_V81 (P = 0.38588 d) and BW2_V8 (P = 0.39402 d). However, the differences in the light curves are quite evident also in these intermediate cases (Fig. 10). The $R_{21} - P$ plot provides the best separation between short–period RRab stars and long–period RRc stars (Fig. 7). While the RRab star displays normal values for its class, the three RRc stars display intermediate values, but always closer to RRc– than to the RRab–type (especially in the $R_{21}-P$ plot). It should be noted that there are few stars in the period interval from 0.35 d to 0.40 d; therefore it is probable that these stars have some particularity.

4. The Fourier diagrams: insights into the different classes

The large number of stars forming each class allows us to discuss some aspects in detail.

4.1. HADS stars

The ϕ_{21} values are quite constant from 0.07 d to 0.20 d, but they show a slight trend to decrease toward shorter periods. For the 11 stars with $P < 0.07$ d, we get $\phi_{21} = 3.92 \pm 0.06$ rad, while for the 28 stars with $0.07 \text{ d} < P < 0.20$ d we get $\phi_{21} = 4.23 \pm 0.04$. This tendency was already noticed in the ω Cen stars (Poretti 1999), where the presence of stars with shorter period (down to 0.036 d) makes the trend more evident. When considering the variables with $P < 0.05$ d, the slope of the $\phi_{21}-P$ progression is not only confirmed, but seems to become steeper again, suggesting a second break (see also Fig. 1 in Poretti 2000b). The change in the slope can also be seen in the $\phi_{31}-P$ and $\phi_{41}-P$ plots, but it is difficult to place it. The gap in the period between 0.080 d and 0.094 d is a further complication. It should be noted that such a gap is not filled by considering variables we excluded for some reason or other: the only star in this interval is the double–mode pulsator BW1_V207.

In correspondence with the break in the $\phi_{21}-P$ progression, Antonello (2000) noted a saddle (centered at P = 0.10 d and flanked by two maxima at 0.08 d and 0.14 d) in the amplitude plots. He correlated this feature with the stage of stellar contraction before the expansion of the envelope. As a matter of fact, the change of slope is unlikely to be due to a resonance effect or a different pulsation mode, which both should produce much more evident changes in the light curves. As regards the latter possibility, we remind the reader of the presence of perfectly sine–shaped light curves in this period range, which could be the signature of an overtone radial mode.

Another feature of interest is the bimodal distribution of the R_{21} values found by Antonello et al. (1986), questioned by Hintz & Joner (1997), re–confirmed by Musazzi et al. (1999), simultaneously weakened by Morgan et al. (1998c) and strengthened by Templeton et al. (1998), to be finally found unclear by Templeton (2000). When plotting the values obtained from the OGLE stars with $P < 0.30$ d (as in the Antonello et al. paper), we observe a bimodal distribution (with different maxima). However,

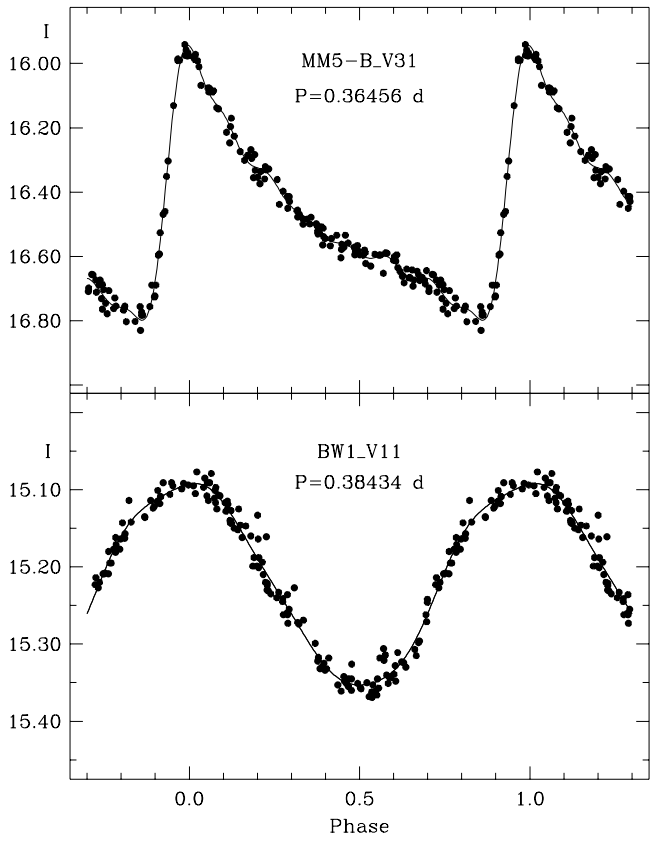

Fig. 10. Top panel: MM5-B_V31 is the RRab star having the shortest period ($P = 0.36456$ d). Bottom panel: BW1_V11 is the RRc star having the longer period ($P = 0.38434$ d). Note also the strong difference in amplitude

when considering the stars with $P < 0.20$ d (i.e. the genuine HADS stars, as previously established), the distribution loses that characteristic, showing a single maximum toward high R_{21} values (Fig. 11). Such high values are required to explain the strongly asymmetric light curves of HADS stars. Therefore, the bimodal distribution is generated by the low R_{21} values typical for RRc stars having short periods, as seen above. This is also confirmed by looking at the Table 2 reported by Antonello et al. (1986): the $R_{21} < 0.20$ values are mostly found in stars with $P > 0.20$ d. As an interesting feedback, this results strengthens our confidence in considering $R_{21} = 0.20$ as the separation between HADS and RRc for periods around 0.20 d.

4.2. RRc stars

There are no peculiarities in the light curves of RRc stars. The only exceptions are the short– and long–period stars which are respectively close to HADS and RRab variables and whose parameters show intermediate values in some cases. The Fourier parameters are well confined in narrow loci in all the plots (Figs. 4, 5, 6 and 7) and their progressions describe very well the main characteristic of these stars, i.e the slow but continuous change in the shape of the light maximum, which appears to be double or flat in

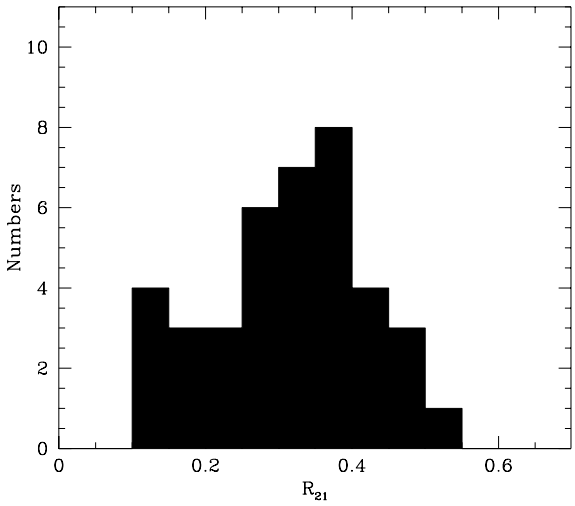

Fig. 11. Histogram of the R_{21} values observed in the light curves of HADS stars. The distribution does not show any peculiarity considering stars with 0.20 d $< P <$ 0.30 d as RRc stars

most cases. When the light curves are more rounded, i.e. around 0.31–0.32 d, there is a corresponding dip in the $R_{31} - P$ and $R_{41} - P$ diagrams.

4.3. RRab stars

The RRab class is richer in particularities than the RRc one. In the phase diagrams there is an unique, narrow progression from 0.40 d to 0.55 d. After this uniform behaviour, we see the ϕ_{i1} values diverge into three "tails". The Fourier ϕ_{41} parameters provide the clearest separation among tails (Fig. 12). The separation is usually larger than 0.50 rad, while the fits of the light curves give a mean error on the ϕ_{41} parameter of 0.16, 0.14 and 0.08 rad for the upper, central and lower tails, respectively. In a few cases, looking at a particular $\phi_{ji} - P$ plot, it is not easy to decide which tail a star belongs to, owing to the error on the phase parameter we are examinating. However, this task can be done in a much more reliable way by considering all the $\phi_{j1} - P$ plots; in that way we take full advantage of the presence of the three tails in each plot. As proven by the three panels in Fig. 12, the same stars form the same type of tail, though with a different degree of clarity. The upper and central tails are merged together for $P < 0.55$ d and cannot be separated; the lower tail originates at $P \sim 0.50$ d. Moreover, the OGLE sample does not contain many stars with $P > 0.65$ d; therefore, this part is not well defined in each tail (see Sects. 5.1 and 5.2).

Once evidenced in the Fourier plots, the differences can be evaluated also by a direct examination of the light curves (Fig. 13):

1. The lower tail is formed by stars having the steepest rising branches and well defined bumps before them; the maxima are sharp and the descending branches are concave (Fig. 13, lower panels). Moreover, there are no great changes when the period increases (compare the

light curve of BW11_V3, $P = 0.596$ d, with that of BW7_V48, $P = 0.639$ d). Stars belonging to this tail can be recovered down to $P = 0.523$ d;

2. The light curves of the stars forming the central tail show a less steep ascending branch; the descending branch has a sort of corrugated shape (Fig. 13, middle panels; note that the points, not the fitting curve, are describing it) for shorter periods (BW9_V14, $P = 0.607$ d) and shows a tendency to become linear for longer periods (BW4_V12, $P = 0.639$ d). Moreover, the bump is wider and less marked than in the lower tail;
3. The upper tail is formed by light curves having the slowest rise to maximum (Fig. 13, upper panels). The bump at minimum light is visible at short periods (BW1_V25, $P = 0.600$ d), but disappears at longer ones (BW8_V20, $P = 0.677$ d); moreover, the descending branch looks convex. The amplitude is smaller than in the two previous cases and a 2nd–order fit is often sufficient. Consequently, the $R_{21} - P$ plot clearly separates the stars belonging to this tail from other RRab variables; in Fig. 7 they originate the points below 0.4 after $P = 0.60$ d.

As the general shape of the curves changes from one tail to another, all the phase parameters are sensitive to differences, particularly the higher–order ones, since they should fit the bump at minimum and the differences in skewness. This explains why the separation of the tails is more conspicuous in the $\phi_{41} - P$ and $\phi_{51} - P$ plots than in the $\phi_{21} - P$ and $\phi_{31} - P$ plots.

5. Discussion

The complete re–analysis of the OGLE database gave us the opportunity to demonstrate the non–existence of the unusual δ Scuti stars reported by Morgan et al. (1998c), to recognize the bimodal distribution of the R_{21} parameters in the HADS sample as a contamination effect, to separate in a better way the three classes of variable stars. Other aspects deserve further discussion, also considering both the inputs needed by theoretical work and the necessity of obtaining clear indications from monoperiodic stars in order to better understand multimode pulsators.

5.1. Features in the progressions

The Fourier parameters are confirmed to be a powerful discriminator between the first overtone mode of RRc stars and the fundamental mode of RRab stars. The same separation is discernible, though with more difficulty, between the RRc stars and the HADS stars, considered to be F mode pulsators. These latter stars show a changing slope at $P \sim 0.10$ d; the possibility of a presence of $1O$ pulsators among short–period HADS is suggested by some sine–shaped light curves and by a small group of stars having high values of ϕ_{21}(Poretti 1999).

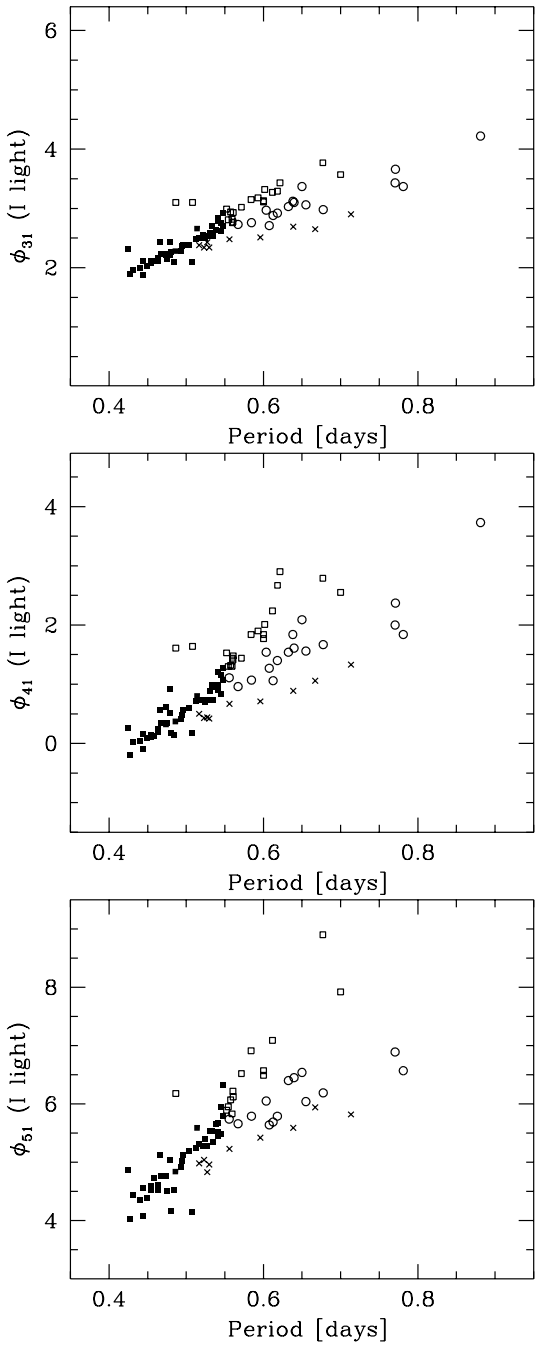

Fig. 12. Fourier ϕ_{31}, $\phi_{41}$and ϕ_{51} parameters of RRab stars in the OGLE database (I light). After a common progression until $P = 0.50-0.55$ d (filled squares), the ϕ_{j1} values diverge into different "tails". The symbols used to identify the three tails are the same as those used in Fig. 13 to plot the different light curves

None of these progressions shows a clear, abrupt change suggesting the presence of a resonance. We can speculate that the upper tail of the RRab changes at $P = 0.64$ d (Fig. 12), as there are two stars (MM5-B_V20 and BW10_V95) showing a R_{21}value and a shape typical of upper sequence stars, but a significantly lower ϕ_{41}value. Moreover, the ϕ_{51} and ϕ_{61} parameters show a regular progression, confirming that the two stars belong to the upper

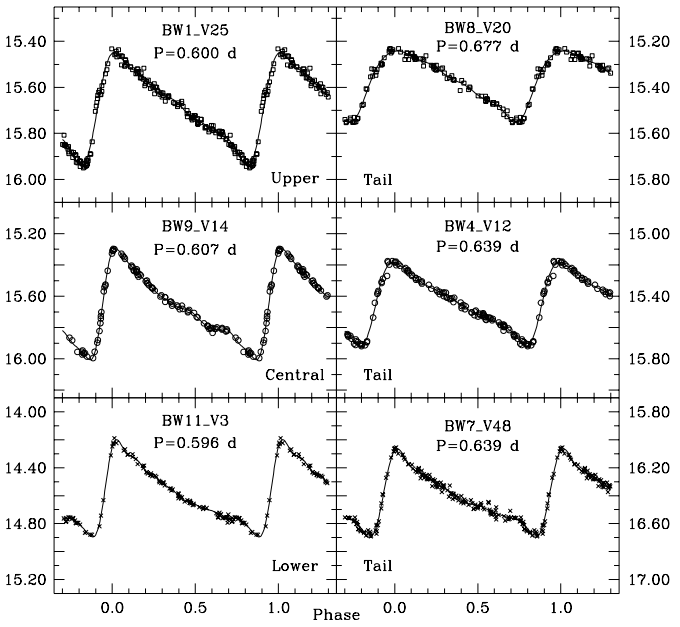

Fig. 13. Light curves of different RRab stars belonging to the three different tails visible in the phase Fourier plots. The upper panels (squares) show a short– and a long–period RRab characterized by high values of the phase differences (upper tail). The central panels (circles) show a short– and a long–period RRab characterized by medium values of the phase differences (central tail). The lower panels (crosses) show a short– and a long–period RRab characterized by low values of the phase differences (lower tail). The RR Lyr variables in each column have approximately the same period and thus differences in the light curve shape at the same period can also be assessed. Note also the differences in the amplitudes

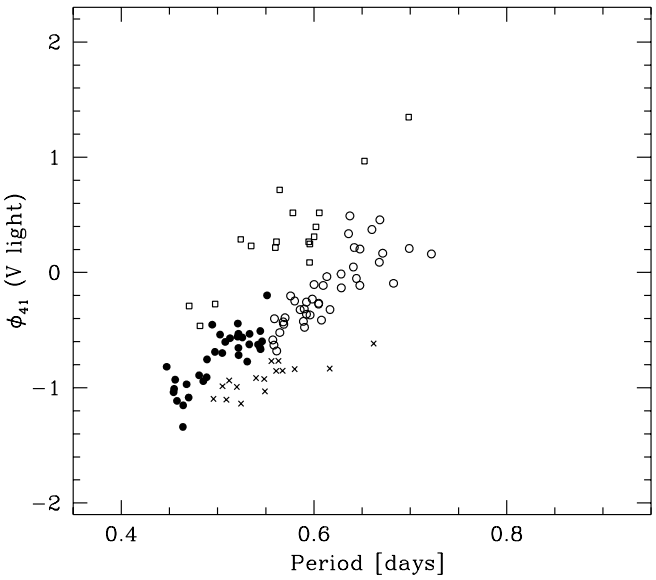

Fig. 14. Fourier ϕ_{41} parameters of RRab stars in some globular clusters (V light). The central tail (filled and open circles) is composed by stars from NGC 6362, M 55, M 9, M 5, NGC 6934 and M 3. The upper tail (open squares) is composed by all the stars from NGC 6171 and few stars from NGC 6362, M 5 and M 3. The lower tail (crosses) indicates stars from M 55 and NGC 6934

tail. It will be interesting to verify the hint of a resonance involving the 3rd overtone by means of a larger database.

5.2. The three tails of the RRab progression

Kovács & Jurcsik (1996, 1997) and Jurcsik (1998) have derived formulae that estimate the absolute magnitudes, metallicities, intrinsic colours and temperatures of RRab stars from the periods, amplitudes and phases. In particular, the [Fe/H] value is related to P and ϕ_{31}. Therefore, the differences in the progression naturally transpose into a difference in metallicity. After transforming the phase differences values from I to V light using the equations provided by Morgan et al. (1998b), we indeed obtained a slightly different mean metallicity: the 20 stars of the upper sequence yield [Fe/H] $= -0.96 \pm 0.04$, the 17 stars of the central one -1.39 ± 0.05 and the 9 stars of the lower one -1.50 ± 0.08. We note that they are strictly monoperiodic pulsators, and the condition of regular light curves (Kovács & Kanbur 1998) is then largely satisfied.

To investigate in more detail the possible effect of the metallicity, we revisited the $\phi_{41} - P$ progression for the RR Lyr variables in NGC 6171 (Clement & Shelton 1997; we omitted two unclear cases), NGC 6362 (Olech et al. 2001), M 3 and M 9 (Clement & Shelton 1999), M 55 (Olech et al. 1999), M 5 (Kaluzny et al. 2000) and NGC 6934 (Kaluzny et al. 2001). We transformed the phase values obtained from a Fourier series in `sin` into phase values from a `cos` series. The parameters obtained in this way are plotted in Fig. 14 using the same symbols as in Fig. 12 to indicate the different tails. Note the sharpness of the OGLE progressions compared with the progressions relative to cluster stars; observations carried out with different instruments and much more crowded fields can explain the larger scatter.

Most of these globular clusters show overlapping central tails (NGC 6362, M 9, M 5 and NGC 6934), despite a large spread in metallicities. However, looking at Table 2 we can see that the expected general distribution is respected: metal-rich globular clusters have some or most stars on the upper tail and none on the lower one, while the RR Lyr stars of the metal–poor clusters populate the lower tail. Note also that the two extreme cases (NGC 6171, metal–rich, and M 55, metal–poor) describe the two progressions well above and below the central one, respectively.

However, all the stars of the same cluster should have the same metallicity and therefore the $\phi_{41} - P$ plot of each cluster should show a single tail, but in three cases we actually observe the co-existence of two kinds of tails (see also Table 1):

1. in M 3 there is a tendency for long–period RRab stars to bend toward higher ϕ_{41}values and to merge in the upper tail (see Clement & Shelton 1999);

Table 2. Distribution of the cluster RRab light curves in the different segments (common part with $P < 0.50$ d and three tails) of the $\phi_{41}-P$ diagrams

Glob. Clus.	[Fe/H]	N	RRab	Tails		
			$P < 0.50$ d	Central $P > 0.50$ d	Upper	Lower
NGC 6362	–0.95	18	11	3	4	–
NGC 6171	–1.04	7	–	–	7	–
M 5	–1.29	30	13	15	2	–
M 3	–1.47	10	2	4	4	–
NGC 6934	–1.54	31	7	10	–	14
M 9	–1.72	6	–	6	–	–
M 55	–1.81	6	1	3	–	2

2. in NGC 6934, the RRab variables with 0.49d $< P <$ 0.56 d seem to belong to the lower sequence and the others to the central one;
3. in NGC 6362 there are some RRab stars with $P >$ 0.60 d belonging to the upper tail and other RRab belonging to the central tail.

Therefore, it looks evident that only the general trend of a large sample can be considered the fingerprint of the metallicity of the cluster, not the Fourier parameters obtained from a few stars.

In the OGLE database the sample is three times more numerous and the separation between the tails looks better defined than in the Clement & Shelton (1999, their Fig. 8) sample. The RRab stars in ω Cen describe a sharp central tail (Poretti 2001, in preparation); a comparison with Fig. 12 supports the hypothesis that the three OGLE stars at $P \sim 0.80$ d belong to this tail.

The presence of the tails in the OGLE database indicates an additional influence apart from metallicity on the light curve shape. We can conjecture that the shapes of the light curves are related to something more general, such as the evolutionary phase, or a combination of different physical conditions, since no obvious metallicity–based segregation is expected for field RR Lyr stars.

5.3. RRc stars

The slope in the $\phi_{31}-P$ plot is steep. The relationships given by Simon & Clement (1993) allowed us to calculate some physical parameters. Morgan et al. (1998b) found a very homogeneous group, with a few stars showing unusual metallicity. We subdivided the RRc sample into two subsets, the first (21 stars) with $0.25 < P < 0.30$ d and the second (17 stars) with $0.30 < P < 0.35$ d. There is no difference in luminosity ($\log L = 1.65 \pm 0.01$ and 1.67 ± 0.01, respectively) and in the relative helium abundance ($Y =$ 0.29 everywhere) between the two subsets. On the other hand, the RRc stars with the shorter period seem more massive (mean mass $0.57 \pm 0.02\ M_\odot$ vs. $0.50 \pm 0.02\ M_\odot$) and hotter (mean temperature $T = 7460 \pm 10$ K vs. $T = 7380 \pm 10$ K), but the differences can be considered marginal. However, this tendency is confirmed when comparing the two RRc variables having $P < 0.25$ d (0.56 and 0.57 $M_\odot$, 7726 K and 7649 K) with the two RRc stars having $P > 0.35$ d (0.58 and 0.78 $M_\odot$, 7177 K and 7047 K).

When considering different globular clusters we note that metallicity is driving the differences in the physical parameters (the mean masses and mean luminosities increase and the mean temperatures and helium abundances decrease with decreasing cluster metal abundance, Clement & Shelton 1997). In the OGLE database and in the same globular cluster (i.e. under the same metallicity), the RRc variables with shorter periods are the more massive and hotter ones (see V2 and V11 in M 55, Olech et al. 1999, or V14 and V28 in NGC 6362, Olech et al. 2000)

This tendency needs to be better fixed by a more robust observational sample, which consider also RRc stars with $P < 0.25$ d (i.e. the extension of the RRc class we introduced here) and RRc stars with $P > 0.35$ d.

5.4. The comparison with the other field RR Lyr stars

Simon & Teays (1982) made the first Fourier decomposition of field RR Lyr stars, including both RRab– and RRc–types (70 stars). Subsequent papers did not further discuss their conclusions. As regards RRab stars, Simon & Teays claimed evidence for a trend, a sort of Cepheid–like progression, for $P > 0.55$ d. This progression is masked by a large scatter, not observed in the OGLE sample. As a consequence, these authors missed the opportunity to note that the progression originated earlier, around $P \sim 0.45$ d and to note the different tails. The reason for such a scatter is unclear, since observational errors or uncertainties on the parameters are not able to explain it fully.

Simon & Teays also emphasized the unusual case constituted by XZ Cet ($P = 0.8231$ d), by far their longest–period star (gap from 0.75 to 0.82 d). The OGLE sample fills such a gap only partially (four stars clustering around 0.77 d) and individuates a longer–period variable, MM7-B_V12 ($P = 0.8812$ d). Considering the whole sample of long–period RRab stars, the general pattern seems to be a continuous progression, not interrupted by any discontinuity, as suggested by Simon & Teays (1982).

We also note that these long–period stars are not found in the globular clusters we considered above: in Fig. 14 the longest period is 0.72 d. As a matter of fact, they seem to characterize metal–rich globular clusters, as NGC 6388 and NGC 6441 (Pritzl et al. 2000).

6. Conclusions

The Fourier coefficients with their error bars are reported in a machine readable form in Table 3 (HADS), Table 4 (RRc) and Table 5 (RRab). Moreover, an atlas of the light curves, least–squares fit and Fourier parameters is available as a ps-file from the author.

The step–by–step analysis we made allowed us to handle a sample characterized in an unambiguous way: no double–mode or Blazhko pulsator, no under– or over–evaluation of the significance of the Fourier components. Consequently, clear outputs have been obtained.

The utility of the Fourier decomposition as a classification tool is confirmed by the segregation of the phase and amplitude parameters in well–defined loci for each class of variables. The use of this technique as a link between observable quantities and stellar physical parameters is demonstrated by the enhanced separations within the same class, as examplified by the three tails in the RRab phase parameter plots. This way of performing the analysis when managing limited samples should give some warnings about the automated analysis of very large samples. A good trade–off could be the introduction of sophisticated checks at intermediate steps.

In a more general way, the exploitation of the large number of light curves supplied by the microlensing projects should be carried out in a careful way, since it can really provide us with the possibility to sound the stellar interiors.

Acknowledgements. Useful comments on a first draft of the manuscript were made by Pawel Moskalik, Siobahn Morgan, Elio Antonello, Geza Kovacs, Christine M. Clement, Giuseppe Bono and the referee, Matthew Templeton. A part of this work was done during a stay at the Copernicus Astronomical Center in Warsaw and the author wishes to thank P. Moskalik and W. Dziembowski for their warm hospitality. An early short visit to Siobahn Morgan at University of Northern Iowa was very helpful in planning this work. The author wishes also to thank J. Vialle for checking English form.

References

Antonello, E. 2000, in Delta Scuti and Related Stars, ed. M. Breger, & M. H. Montgomery, ASP Conf. Ser., N. 210, 381
Antonello, E., Broglia, P., Conconi, P., & Mantegazza, L. 1986 A&A, 169, 122
Carpino, M., Milani, A., & Nobili, A. M. 1987, A&A, 181, 182
Clement, C. M., & Shelton, I. 1997, AJ, 113, 1711
Clement, C. M., & Shelton, I. 1999, AJ, 118, 453
Feuchtinger, M., Buchler, J. R., & Kolláth, Z. 2000, ApJ, 544, 1056
Hintz, E. G., & Joner, M. D. 1997, PASP, 109, 639
Jurcsik, J. 1998, A&A, 333, 571
Kaluzny, J., Olech, A., Thompson, I. B., et al. 2000, A&AS, 143, 215
Kaluzny, J., Olech, A., & Stanek, K. Z. 2001, AJ, 121, 1533
Kienzle, F., Moskalik, P., Bersier, D., & Pont, F. 1999, A&A, 341, 818
Kovács, G., & Jurcsik, J. 1996, ApJ, 466, L17
Kovács, G., & Jurcsik, J. 1997, A&A, 322, 218
Kovács, G., & Kanbur, S. 1998, MNRAS, 295, 834
Morgan, S. M., Simet, M., & Bargenquast, S. 1998a, Acta Astron., 48, 331
Morgan, S. M., Simet, M., & Bargenquast, S. 1998b, Acta Astron., 48, 341
Morgan, S. M., Simet, M., & Bargenquast, S. 1998c, Acta Astron., 48, 509
Musazzi, F., Poretti, E., Covino, S., & Arellano-Ferro, A. 1999, PASP, 110, 1156
Olech, A., Kaluzny, J., Thompson, I. B., et al. 1999, AJ, 118, 442
Olech, A., Kaluzny, J., Thompson, I. B., et al. 2001, MNRAS, 321, 421
Pardo, I., & Poretti, E. 1997, A&A, 324, 121
Poretti, E. 1999, A&A, 346, 487
Poretti, E. 2000a, in Variable Stars as Essential Astrophysical Tools, ed. C. Ibanoglu, NATO ASI Ser. C, 544, 421
Poretti, E. 2000b, in Variable Stars as Essential Astrophysical Tools, ed. C. Ibanoglu, NATO ASI Ser. C, 544, 227
Pritzl, B., Smith, H. A., Catelan, M., & Sweigart, A. V. 2000, ApJ, 530, L41
Simon, N. R., & Clement, C. M. 1993, ApJ, 410, 526
Simon, N. R., & Teays, T. T. 1982, ApJ, 261, 586
Templeton, M. R. 2000, Delta Scuti Newsletter, 14, 16
Templeton, M. R., McNamara, B., & the MACHO team, 1998, Delta Scuti Newsletter, 12, 18
Udalski, A., Szymanski, M., Kaluzny, J., et al. 1993, Acta Astron., 43, 289